

“Nanoscale Lattice Fence” in a Metal–Organic Framework: Interplay between Hinged Topology and Highly Anisotropic Thermal Response

Lucas D. DeVries,[†] Paul M. Barron,[†] Evan P. Hurley,[†] Chunhua Hu,[‡] and Wonyoung Choe^{*,†,§}

[†]Department of Chemistry and [§]Nebraska Center for Materials and Nanoscience, University of Nebraska-Lincoln, Lincoln, Nebraska 68588-0304, United States

[‡]Department of Chemistry, New York University, New York, New York 10003-6688, United States

 Supporting Information

ABSTRACT: A thermoresponsive, 3D hinged metal–organic framework (HMOF-1) assembled from *meso*-tetra(4-pyridyl)porphine and CdI₂ exhibits a 3D “lattice fence” topology with extraordinary thermal expansion and shrinkage. A simple structural model is established to elucidate such a drastic thermal response. The hinged structure model presented here can also be applied to other “lattice fence” topologies with little or no modification, depending on the symmetry of the molecular building blocks.

When temperature rises, most solid-state materials expand, while some materials shrink; these phenomena are known as positive and negative thermal expansion, respectively.^{1,2} Such macroscopic expansion or shrinkage upon heating often stems from collective atomic-scale movements such as bending and stretching vibrations. Typically, positive thermal expansion coefficients for solid-state materials such as metals and ceramics fall in the range $(1–20) \times 10^{-6} \text{ K}^{-1}$.^{1,3} Recent developments in this area include several self-assembled frameworks, which are emerging as a new class of thermoresponsive materials. Few of these materials exhibit “colossal” thermal expansion coefficients greater than $100 \times 10^{-6} \text{ K}^{-1}$, as exemplified by Ag₃[Co(CN)₆] and its related Prussian blue analogues.^{4–6} The detailed mechanism of colossal thermal expansion becomes a fascinating subject of study because the origin of such extreme thermal expansion is fundamentally different from that found in other “normal” solid-state materials.^{4–7} A detailed understanding of this matter at the atomic or molecular level may provide key information on new design principles for thermoresponsive frameworks for devices in sensors, actuators, and other applications.^{2,8,9}

In this communication, we report a new thermoresponsive three-dimensional (3D) hinged metal–organic framework HMOF-1 (HMOF stands for *hinged metal–organic framework*). The structure resembles a 3D nanoscale “lattice fence”. HMOF-1 shows a colossal thermal expansion coefficient of ca. $+177 \times 10^{-6} \text{ K}^{-1}$ over the temperature range 160–320 K, which is among the highest values reported for framework solids. Such extreme thermal expansion is due to hinged movement around the metal nodes in HMOF-1.

HMOF-1 is assembled from *meso*-tetra(4-pyridyl)porphine and CdI₂. Figure 1 shows the single-crystal structure of HMOF-1 at 100 K.^{10,11} In this structure, each cadmium atom is coordinated equatorially to four pyridyl groups of the neighboring

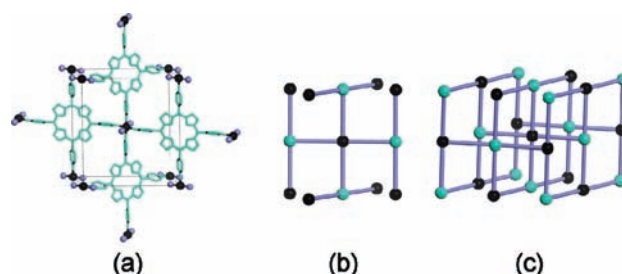


Figure 1. (a) Single-crystal structure of HMOF-1 at 100 K. (b) Simplified structure showing two types of four-connected nodes, cadmium (black) and the porphyrin centroid (turquoise). (c) Expansion of (b) to relate the *cds* topology.

porphyrins and axially to two iodide anions, forming an octahedral coordination geometry.¹⁰ Closer examination of the structure of HMOF-1 reveals that the framework adopts the CdSO₄ (*cds*) topology, a four-connected 3D net.^{12,13} It is interesting to note that unlike other *cds*-type MOFs, HMOF-1 is a rare example of a *cds*-type framework that is not interpenetrated.¹⁴

The *cds* topology can be derived from the NaCl structure by deleting one-third of the connections between the nodes [see Figure S1 in the Supporting Information (SI)]. Although the *cds* topology has significantly fewer connections than the parent NaCl structure, it has the same number of nodes. Interestingly, the rigid nature of the NaCl topology is no longer maintained in the *cds* topology, as a structural model of the *cds* net appears to be quite flexible (see the movie in the SI). We notice hinged movement around the metal nodes in this structure model. Similar hinged movement in the framework topology is well-recognized in *ths*-type structures.¹⁵ Such hinged frameworks have been shown to have unusual mechanical and thermal properties originating from the structural feature that the entire lattice can undergo a nearly barrierless twisting motion around the parallel nodes.¹⁵ However, unlike *ths*-type structures, the hinged nature of the *cds* topology has not been explicitly addressed in the literature, despite the fact that a few *cds*-type structures have already been reported to be flexible upon guest removal and uptake.¹⁶

Since HMOF-1 adopts the *cds* topology, we hypothesized that HMOF-1 could be a hinged framework that would respond to heating or other external stimuli. To verify this hypothesis, we

Received: April 9, 2011

Published: August 30, 2011

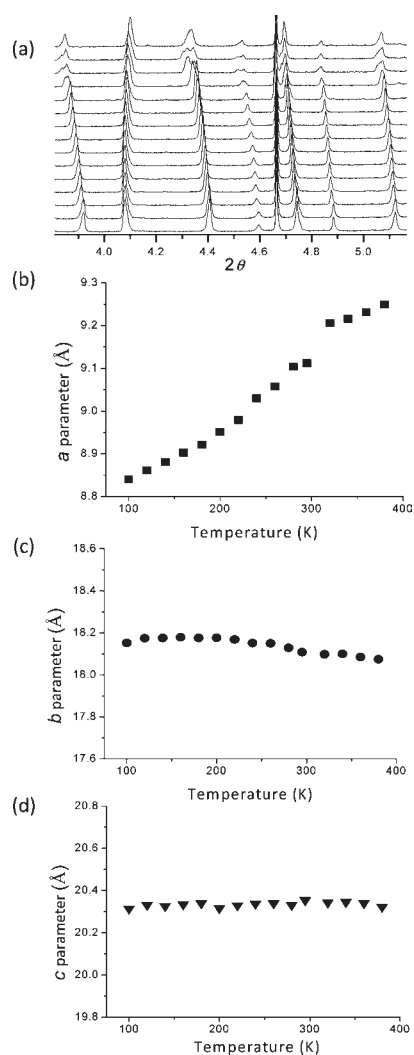


Figure 2. Temperature-dependent (a) synchrotron PXRD patterns and (b–d) unit cell parameters *a*, *b*, and *c*, respectively.

performed temperature-dependent single-crystal X-ray diffraction experiments at higher temperatures (e.g., 200 and 297 K) together with synchrotron powder X-ray diffraction (PXRD) experiments over the temperature range 100–380 K.¹⁷ A gradual structural transformation upon heating can be clearly seen in the synchrotron PXRD data (Figure 2a), where some reflections are shifted toward lower or higher values of 2θ , indicating a structural transformation of HMOF-1.

The unit cell parameter data for HMOF-1 show an interesting temperature-dependent behavior (Figure 2b–d). These data support the flexible nature of HMOF-1. Notably, the *a* parameter undergoes the most drastic change upon heating. To our surprise, over a 280 K temperature range, *a* increases by nearly 5%! In contrast, *b* decreases by 0.5% and *c* remains relatively unchanged (Figure S3). The single-crystal data also show the same trend (Table S1). Thermal expansion coefficients (α) along the *a* and *b* directions were calculated using X-ray synchrotron data. The mean value of α_a for HMOF-1 over the temperature range 160–320 K is ca. $+177 \times 10^{-6} \text{ K}^{-1}$, demonstrating positive colossal thermal expansion, (i.e., $|\alpha| \geq 100 \times 10^{-6} \text{ K}^{-1}$). This value is comparable to other highest values reported for framework solids.^{4,18}

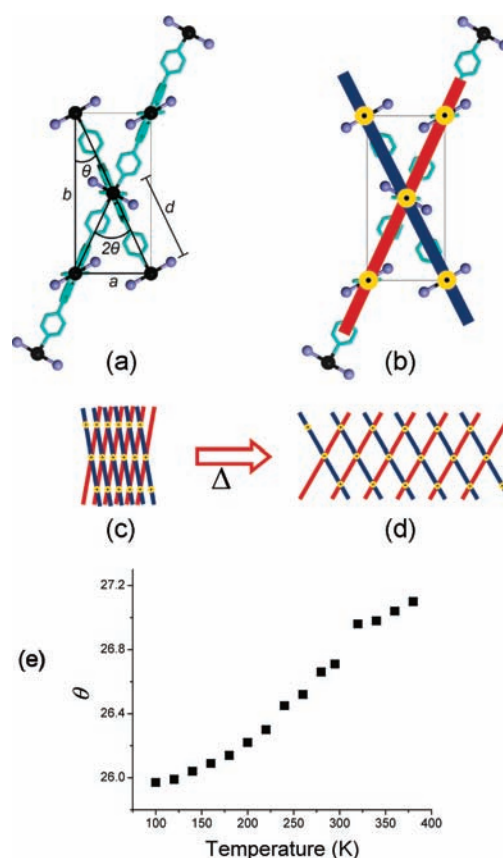


Figure 3. (a, b) Crystal structure of HMOF-1 (a) viewed along the [001] direction showing the hinge angle θ and (b) further simplified to show porphyrin bars (red and blue) of a “lattice fence” with cadmium atoms (yellow) as pivoting points. (c, d) Illustration of the “lattice fence” showing hinged expansion in going from (c) to (d). (e) Plot of the hinge angle θ as a function of temperature.

It is noteworthy that there is negative thermal expansion behavior along the *b* direction upon heating, i.e., $\alpha_b = -21 \times 10^{-6} \text{ K}^{-1}$ at 160–320 K. Therefore, the thermal response of HMOF-1 is highly anisotropic, with positive colossal thermal expansion behavior along the *a* direction coupled to negative thermal expansion in the perpendicular *b* direction, similar to the cases known for $\text{Ag}_3[\text{Co}(\text{CN})_6]$ and its derivatives.⁴ To test the reversibility of the hinged movement, the cell parameter data were collected from 297 to 380 K and then back to 297 K, where they showed a complete return to the original cell parameters.

Figure 3a illustrates another structural representation of HMOF-1 that can be used to analyze the flexibility of HMOF-1 and its relationship with the *cds* topology. The hinge angle θ shown in Figure 3a is significantly smaller than that of an ideal *cds* net (45°).¹⁹ The structure of HMOF-1 can be compared to that of a simple “lattice fence”, with cadmium atoms serving as pivoting points (Figure 3b). The angle θ is a key parameter for the flexibility of HMOF-1. Interestingly, because of the orthorhombic symmetry of the space group *Pnmm* to which HMOF-1 belongs, the *a* and *b* cell parameters of HMOF-1 can be expressed by simple trigonometric formulas involving two geometric parameters, the angle θ and the distance *d* between two four-connected nodes, namely, the cadmium and the porphyrin centroid (Figure 3a). These formulas are $a = 2d \sin \theta$ and $b = 2d \cos \theta$. According to these relationships, as θ increases, the *a*

and b parameters show positive and negative thermal expansions, respectively, when $\theta < 45^\circ$, in agreement with the trend found in the experimental data in Figure 2.

Perhaps the most notable feature of HMOF-1 is that the θ value changes by ca. 1.1° over the entire temperature range 100–380 K (Figure 3e). The structural model can also be used to calculate θ_{\min} in HMOF-1, which can be expressed as $\theta_{\min} \approx \arcsin[(l_1 + l_2)/(d^2 + 4l_1^2)^{1/2}]$, where l_1 and l_2 are the Cd–I distance (2.94 Å) and half of the I···I distance, respectively (see Figure S6). The angle θ_{\min} was estimated as 25.8° , which compares well with the value of 25.5° obtained from the single-crystal data at 100 K, indicating that HMOF-1 at this temperature is nearly at its minimum θ value. This structural model also shows that the length of the organic linker (d) and the distance to the axial coordinating anion (l_2) are two important parameters for the thermal expansion of this compound and similar cds-type framework solids.

It appears that the hinged motion in HMOF-1 originates from expansion of the interaction between two adjacent iodides attached to cadmium metal nodes. On the basis of the single-crystal data, we indeed detected a noticeable change in $d(\text{I} \cdots \text{I})$, which ranged from 4.43 Å at 100 K to 4.50 Å at 200 K and 4.69 Å at 297 K. As temperature increased, $d(\text{I} \cdots \text{I})$ increased, making the Cd–I bonds cooperatively rotate along the c axis to amplify the mechanical response. An analogous phenomenon has been found in $\text{Ag}_3[\text{Co}(\text{CN})_6]$, where the argentophilic interaction is responsible for its colossal thermal expansion.⁴

Snurr and co-workers showed that interpenetration has a negative effect on the magnitude of the thermal expansion coefficient α .⁸ The change in one of the cell parameters for the non-interpenetrated framework was nearly an order of magnitude greater than that for the doubly interpenetrated framework.⁸ The fact that HMOF-1 is non-interpenetrated might be helpful in generating the colossal thermal expansion. An important structural feature of this hinged framework is that the coordination environment of the metal nodes do not change. Despite the hinged motion, the octahedral coordination geometry of the Cd metal nodes remains the same. Hinged movement is also noted in minerals, as exemplified by tenorite and synthetic melanothalite, Cu_2OCl_2 .²⁰

The mechanism of thermal expansion observed in HMOF-1 resembles expansion and shrinkage of a “lattice fence” and differs considerably from the mechanism in other conventional thermal expansion materials. For example, in the case of metal oxides, the transverse vibration mode of O–M–O (or M–O–M') bonds are responsible for negative thermal expansion.²¹ However, in the case of HMOF-1, bond stretching or bending around the metal node is not responsible for the extraordinary expansion and shrinkage observed. Instead, a hinged motion around the cadmium metal node causes this colossal thermal expansion, as confirmed by single-crystal X-ray and synchrotron PXRD data. This “lattice fence” structural model for the cds topology can be applied to other hinged frameworks with little or no modification.

In summary, we have reported a new thermoresponsive framework solid, HMOF-1, whose topology is similar to a hinged lattice fence. A highly anisotropic thermal response originates from this unique hinged net topology. Other external stimuli (e.g., pressure) might cause similar flexible movement in HMOF-1.

■ ASSOCIATED CONTENT

Supporting Information. Movie (AVI) showing the flexible cds topology, experimental procedures, single-crystal X-ray

and synchrotron PXRD data, coefficients of thermal expansion, flexible model calculations, and CIF files. This material is available free of charge via the Internet at <http://pubs.acs.org>.

■ AUTHOR INFORMATION

Corresponding Author
choe2@unl.edu

■ ACKNOWLEDGMENT

We thank the University of Nebraska-Lincoln for support of this research and Dr. Matthew Suchomel at Argonne National Laboratory for synchrotron experiments. Use of the Advanced Photon Source at Argonne National Laboratory was supported by the U.S. Department of Energy, Office of Science, Office of Basic Energy Sciences, under Contract DE-AC02-06CH11357.

■ REFERENCES

- (1) Krishnan, R. S.; Srinivasan, R.; Devanarayanan, S. *Thermal Expansion of Crystals*; Pergamon: Oxford, U.K., 1979.
- (2) For reviews of negative thermal expansion, see: (a) Miller, W.; Smith, C. W.; Mackenzie, D. S.; Evans, K. E. *J. Mater. Sci.* **2009**, *44*, 5441. (b) Evans, J. S. O. *J. Chem. Soc., Dalton Trans.* **1999**, 3317.
- (3) The linear thermal expansion coefficient α_l is defined as $\Delta(\ln l)/\Delta T$, where l and T are length and temperature, respectively.²
- (4) Goodwin, A. L.; Calleja, M.; Conterio, M. J.; Dove, M. T.; Evans, J. S. O.; Keen, D. A.; Peters, L.; Tucker, M. G. *Science* **2008**, *319*, 794.
- (5) (a) Goodwin, A. L.; Kennedy, B. J.; Kepert, C. J. *J. Am. Chem. Soc.* **2009**, *131*, 6334. (b) Korcok, J. L.; Katz, M. L.; Lenzhoff, D. L. *J. Am. Chem. Soc.* **2009**, *131*, 4866.
- (6) Phillips, A. E.; Halder, G. J.; Chapman, K. W.; Goodwin, A. L.; Kepert, C. J. *J. Am. Chem. Soc.* **2010**, *132*, 10.
- (7) (a) Férey, G.; Serre, C. *Chem. Soc. Rev.* **2009**, *38*, 1380. (b) Liu, Y.; Her, J.-H.; Dailly, A.; Ramirez-Cuesta, A. J.; Neuman, D. A.; Brown, C. M. *J. Am. Chem. Soc.* **2008**, *130*, 11813. (c) Das, D.; Jacobs, T.; Barbour, L. J. *Nat. Mater.* **2010**, *9*, 36.
- (8) Dubbeldam, D.; Walton, K. S.; Ellis, D. E.; Snurr, R. Q. *Angew. Chem., Int. Ed.* **2007**, *46*, 4496.
- (9) Han, S. S.; Goddard, W. A., III. *J. Phys. Chem. C* **2007**, *111*, 15185.
- (10) For examples of framework solids assembled from meso-tetra-(4-pyridyl)porphine building blocks and Cd metal nodes, see: (a) Abrahams, B. F.; Hoskins, B. F.; Robson, R. *J. Am. Chem. Soc.* **1991**, *113*, 3606. (b) Sharma, C. V. K.; Broker, G. A.; Huddleston, J. G.; Baldwin, J. W.; Metzger, R. M.; Rogers, R. D. *J. Am. Chem. Soc.* **1999**, *121*, 1137. (c) DeVries, L. D.; Choe, W. *J. Chem. Crystallogr.* **2009**, *39*, 229.
- (11) For details of the single-crystal X-ray and PXRD data for HMOF-1, see the SI.
- (12) Friedrichs, O. D.; O'Keeffe, M.; Yaghi, O. M. *Solid State Sci.* **1996**, *5*, 73.
- (13) The cds net is one of the most popular nets in framework solids. See: Carlucci, L.; Ciani, G.; Proserpio, D. M. *Chem. Commun.* **2004**, 380.
- (14) Because of the self-duality of the cds net,¹¹ most cds-type frameworks are interpenetrated. See: (a) Zheng, N.; Zhang, J.; Bu, X.; Feng, P. *Cryst. Growth Des.* **2007**, *7*, 2576. (b) Shin, D. M.; Lee, I. S.; Chung, Y. K.; Lah, M. S. *Chem. Commun.* **2003**, 1036. (c) Bhogala, B. R.; Thallapally, P. K.; Nangia, A. *Cryst. Growth Des.* **2004**, *4*, 215. For examples of non-interpenetrated cds-type frameworks, see: (d) Thirumurugan, A.; Natarajan, S. *Cryst. Growth Des.* **2006**, *6*, 983.
- (15) The ThSi_2 (ths) topology is another hinged framework. See: Gardner, G. B.; Venkataraman, D.; Moore, J. S.; Lee, S. *Nature* **2002**, *374*, 792.
- (16) For an example of a flexible cds-type framework, see: Niel, V.; Thompson, A. L.; Munoz, C.; Galet, A.; Goeta, A. E.; Real, J. A. *Angew. Chem., Int. Ed.* **2003**, *42*, 3760.

(17) Temperature-dependent PXRD scans were conducted at the 11-BM beamline at Argonne National Laboratory. See the following website: <http://11bm.xor.aps.anl.gov/description.html> (accessed April 9, 2011).

(18) Yang, C.; Wang, X.; Omary, M. A. *Angew. Chem., Int. Ed.* **2009**, *48*, 2500.

(19) The angle θ was calculated from the relationship $\tan \theta = a/b$.

(20) (a) Krivovichev, S. V.; Filatov, S. K.; Burns, P. C. *Can. Mineral.* **2002**, *40*, 1185. (b) Domnina, M. I.; Filatov, S. K.; Zyzyukina, I. I.; Vergasova, L. P. *Neorg. Mater.* **1986**, *22*, 1992.

(21) Mary, T. A.; Evans, J. S. O.; Vogt, T.; Sleight, A. W. *Science* **1996**, *272*, 90.